

- [4] A. Von Hippel, *Dielectric Materials and Applications* New York: Wiley, 1954, ch. 2.
- [5] S. S. Stuchly and M. Hamid, "Physical parameters in microwave heating processes," *J. Microwave Power*, vol. 7, no. 2, figs. 5 and 6, p. 124, 1972.
- [6] F. Gardiol and O. Parriaux, "Excess losses in *H*-plane loaded waveguide," *IEEE Trans. Microwave Theory Tech.*, vol. 21, pp. 457-461, July 1973.
- [7] J. Ness, "Broadband permittivity measurements at microwave frequency," *IREE Dig. (Australia)*, pp. 330-332, Sept. 1983.
- [8] R. E. Collin, *Field Theory of Guided Wave*. New York: McGraw Hill, 1960.

## Design Curves for -3-dB Branchline Couplers

A. F. CELLIERS AND  
J. A. G. MALHERBE, SENIOR MEMBER, IEEE

**Abstract** — Design curves for -3-dB branchline couplers that include compensation for the junction discontinuities are presented. The curves are obtained by including an accurate model of a stripline *T*-junction in an optimization program.

### I. INTRODUCTION

The performance of -3-dB branchline couplers can be severely degraded by junction effects due to finite line widths. With increasing frequency, line widths become larger relative to line lengths and the junction effects become progressively more severe. The junction effects have been described by several authors [1]-[5]. Dydyk [6] compensates for the effects of the junctions by modifying the line lengths and both impedance levels of a branchline coupler; Cuhaci and Lo [7] compensate for these effects by the introduction of compensating stubs and impedance level changes. Chadha and Gupta compensate for discontinuities by cutting a small notch in the line [8].

An accurate equivalent circuit for the junction was obtained by comparing the predictions from [1]-[6] with a constructed coupler, and the junction properties thus obtained were used in an equivalent circuit of the branchline coupler. For each frequency of interest, and for a number of typical substrates for stripline realization, a computer optimization program was run to compute new branchline lengths and impedance levels that, together with the junction effect, will yield the correct amount of coupling at the desired center frequency.

### II. EQUIVALENT CIRCUIT

A test coupler was fabricated at 2.5 GHz on 1/8-in GPS Polyguide and the coupler properties measured. This was compared to predictions based on the junction equivalents of [1]-[6], and it was found that, in most cases, strong deviation from the measured responses occurred. As an example, the prediction based on the model of [3] is shown in Fig. 1.

Fig. 1 also shows the measured response of the coupler, as well as the theoretical prediction, obtained with a modified version of

Manuscript received November 14, 1984; revised May 6, 1985. This paper is based on a dissertation by A. F. Celliers submitted to the Department of Electrical and Electronic Engineering, University of Stellenbosch, South Africa, in partial fulfillment of the requirements of the M. Eng. degree.

A. F. Celliers is with the National Institute for Aeronautics and Systems Technology, Council for Scientific and Industrial Research, Pretoria, South Africa.

J. A. G. Malherbe is with the Department of Electronic Engineering and Laboratory for Advanced Engineering, University of Pretoria, South Africa.

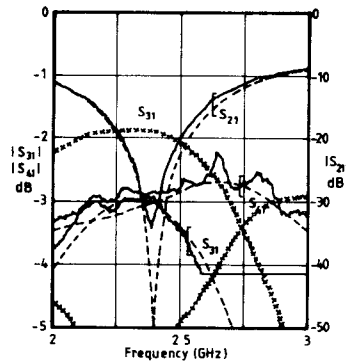


Fig. 1. Measured (solid line) and predicted (dotted line) response of uncompensated coupler.

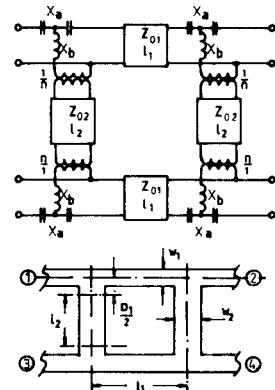


Fig. 2. Equivalent circuit of coupler including junction discontinuities.

the equivalent circuit described in [5], obtained by rearranging the equations. Referring to Fig. 2

$$n = \frac{n' \cos\left(\frac{2\pi}{\lambda_g} \cdot d'_{[WGH]}\right)}{\cos\left(\frac{2\pi d}{\lambda_g}\right)} \quad (1)$$

$$\tan\left(\frac{2\pi}{\lambda_g} d'_{[WGH]}\right) = \frac{Z_{01}}{Z_{02}} (n')^2 \frac{X_b}{Z_{01}} \quad (2)$$

$$\tan\left(\frac{2\pi d}{\lambda_g}\right) = \frac{-X_a}{Z_{01}} \quad (3)$$

$$n' = \frac{\sin(\pi D_2 / \lambda_g)}{\pi D_2 / \lambda_g} \quad (4)$$

$$n_1 = n' \sqrt{Z_{01} / Z_{02}} \quad (5)$$

$$\frac{X_a}{Z_{01}} = \frac{-D_2}{\lambda_g} [0.785 n_1]^2 \quad (6)$$

where  $d'_{[WGH]}$  is obtained from [9]. The parameter  $d$  is calculated from (3), and defined in Fig. 2.

From [2], calculate

$$D_t = \begin{cases} w_t + \frac{2b \ln 2}{\pi} + \frac{t}{\pi} \left[ 1 - \ln \left( \frac{2t}{b} \right) \right], & \text{for } \left( \frac{w_t}{b} \right) > 0.5 \\ b \frac{K(k)}{K(k')} + \frac{t}{\pi} \left[ 1 - \ln \left( \frac{2t}{b} \right) \right], & \text{otherwise} \end{cases} \quad (7)$$

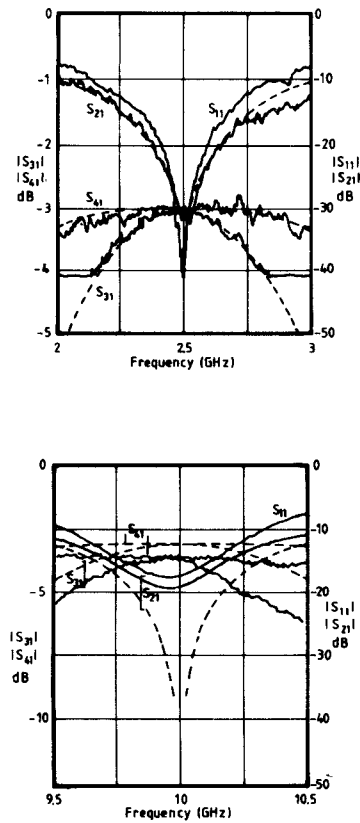


Fig. 3. (a) Measured (solid line) and calculated (dotted line) responses for an optimized coupler at 2.5 GHz and (b) 10.0 GHz.

TABLE I  
COMPARISON OF DIMENSIONS OF NORMALLY DESIGNED AND  
OPTIMIZED COUPLERS

FREQUENCY (GHz)	$Z_1$ ( $\Omega$ )	$Z_2$ ( $\Omega$ )	$l_1$ (mm)	$l_2$ (mm)
Normal Design	2.5	50.0	35.4	19.7
		50.0	35.0	16.6
Optimized Design	10.0	50.0	35.4	14.4*
		50.0	33.7	12.9*

\*  $\frac{3}{4}\lambda_g$  - design

where

$$i = 1, 2$$

$$k = \tanh\left(\frac{\pi w_i}{2b}\right) \quad (8)$$

$$k' = \sqrt{1 - k^2} \quad (9)$$

and  $K(k)$  is an elliptic integral of the first kind.

### III. COMPUTER OPTIMIZATION

The line lengths and characteristic impedance levels of the equivalent circuit were optimized in a computer program using (1)–(6); the curve for  $d'$  from [9] was incorporated as a lookup table. The optimization was carried out for equal power split and isolation simultaneously.

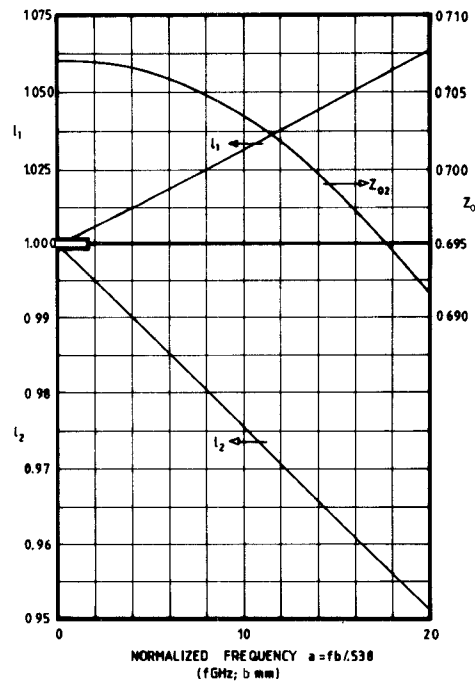


Fig. 4. Design curves for  $-3$ -dB branchline couplers.

Fig. 3 shows the measured and calculated responses for optimized couplers at 2.5 and 10.0 GHz. The agreement between the calculated and measured results at 2.5 GHz are better than 0.1 dB. The difference between the measured and predicted responses at 10 GHz of 0.3 dB is due solely to loss, which was not taken into consideration in the computer optimization program. In both cases the power split is better than 0.1 dB. The dimensions of the optimized and conventional designs are compared in Table I.

### IV. DESIGN CURVES

The procedure described above was repeated for a number of different combinations of material and ground plane spacing, each time varying the design frequency. It was found that, for a large variety of ground plane spacings,  $3.175 \leq b \leq 0.508$  mm, and for values of  $\epsilon_r$  between 2.32 and 2.45, the design curves can be presented as universal curves. The values for  $Z_2$  is accurate to within 0.2 percent over the entire range, and the lengths  $l_1$  and  $l_2$  to within 0.35 and 0.2 percent, respectively. These errors cause an imbalance of less than 0.1 dB in coupling.

The normalized curves are shown in Fig. 4; from it, line impedances and lengths can be read off directly. The impedances are normalized to  $50 \Omega$ , and the line lengths to  $\lambda_g/4$ .

### V. CONCLUSION

A design procedure for  $-3$ -dB branchline couplers that compensates for junction effects has been described. Measurements up to 10 GHz correlate extremely well with the predicted performance.

### VI. ACKNOWLEDGMENT

The authors wish to express their appreciation to the reviewer who suggested normalizing the curves.

## REFERENCES

- [1] A. A. Oliner, "Equivalent circuits for discontinuities in balanced strip transmission lines," *IRE Microwave Theory Tech.*, vol. MTT-3, pp. 134-143, Mar. 1956.
- [2] H. M. Altschuler and A. A. Oliner, "Discontinuities in the centre conductor of symmetric strip transmission line," *IRE Trans. Microwave Theory Tech.*, vol. MTT-8, pp. 328-339, May 1960.
- [3] I. J. Bahri and R. Garg, "A designer's guide to stripline circuits," *Microwaves*, vol. 17, no. 1, pp. 90-96, Jan. 1978.
- [4] W. H. Leighton, Jr., and A. G. Milnes, "Junction reactance and dimensional tolerance effects on X-band, -3 dB directional couplers," *IEEE Trans. Microwave Theory Tech.*, vol. MTT-19, pp. 818-824, Oct. 1971.
- [5] A. G. Franco and A. A. Oliner, "Symmetric strip transmission line tee junction," *IRE Trans. Microwave Theory Tech.*, vol. MTT-10, pp. 118-124, Mar. 1962.
- [6] M. Dydik, "Master the T-junction and sharpen your MIC designs," *Microwaves*, vol. 16, no. 5, pp. 184-186, May 1977.
- [7] M. Cuhaci and G. J. P. Lo, "High frequency microstrip branch-line coupler design with T-junction discontinuity compensation," *Electron Lett.*, vol. 17, no. 2, pp. 87-89, Jan. 22, 1981.
- [8] R. Chadha and K. C. Gupta, "Compensation of discontinuities in planar transmission lines," *IEEE Trans. Microwave Theory Tech.*, vol. MTT-30, pp. 2151-2155, Dec. 1982.
- [9] N. Marcuvitz, *Waveguide Handbook* (MIT Radiation Lab Series, vol. 10). New York: McGraw-Hill, 1949, pp. 336-339, 344-347, 363-368.

## Power Increase of Pulsed Millimeter-Wave IMPATT Diodes

R. PIERZINA AND J. FREYER

**Abstract** — The fabrication and encapsulation of single-drift pulsed IMPATT diodes for 73 GHz is described. The transforming properties of the parasitic inductance and capacitance demonstrate the strong influence of diode-mounting technique. The used reduced-height waveguide resonator is described theoretically, giving an indication of optimum matching between resonator and transformed diode impedance. The diodes deliver more than 10-W output power at 73 GHz with 5-percent efficiency, if they are matched to the resonator by proper parasitics.

### I. INTRODUCTION

At millimeter-wave frequencies, there is great interest in solid-state transmitters for radar, radiometry, or short-range communication systems. The high-power pulsed IMPATT diode has been proven to be the key element for these applications. Besides exact controllable semiconductor technology, packaging and circuit-mounting techniques are important factors for optimum performance. At microwave frequencies up to the *Ku*-band, semiconductor elements are either mounted in sealed metal-ceramic packages or are bonded directly into the microwave circuit [1], [2]. In contrast to these frequencies where the packaging technique normally will not limit the RF performance, the mounting parasitics at millimeter waves cause a transformation of the active diode impedance and usually limit output power and efficiency [1], [3]. Therefore, it is important to minimize the resistive parasitics associated with the diode chip and its mounting connections. The use of package parasitics for impedance matching [4], [5], however, shows that the often-stated demand of minimum parasitics [5], [6] does not lead automatically to the best RF performance results.

In this paper, design and fabrication of high-power pulsed IMPATT diodes for upper *V*-band frequencies are described. The

Manuscript received May 31, 1984; revised May 15, 1985. This work was supported in part by Fraunhofer-Gesellschaft (FHG).

The authors are with the Technische Universität München, Lehrstuhl für Allgemeine Elektrotechnik und Angewandte Elektronik, Arcisstraße 21, D-8000 München 2, West Germany.

output-power optimization is demonstrated by way of a single-drift diode because, in contrast to double-drift structures, only one active layer has to be adjusted. This, however, can easily be done by technological means [7]. The load impedance of the used resonator with reduced height is described in detail [8], representing the influence of the tuning elements. Since the diode impedance is transformed by the parasitic mounting capacitance and lead inductance, different encapsulation techniques of the diode are investigated. It is shown, that more than 10-W peak output power with 5-percent efficiency can be obtained if the diode impedance is well matched to the used resonator by proper parasitics.

### II. DEVICE FABRICATION

Initial material for the pulsed single-drift IMPATT diode is n-n<sup>+</sup> epitaxial silicon with a doping concentration of  $6 \times 10^{16}$  cm<sup>-3</sup> of the n layer with thickness of 0.8  $\mu$ m. The p-n junction is formed by a shallow boron diffusion resulting in a 0.55- $\mu$ m-thick active layer designed for optimum frequencies in the upper *V*-band. The punch-through factor of the diodes is 1.8. The highly doped substrate is reduced by bubble etching to a thickness of only 1 or 2  $\mu$ m in order to minimize losses due to the diode series resistance. This very thin substrate layer is also advantageous for short-pulse application of the diodes. In this case, the increase of the diode temperature during the current pulse is reduced as the heat flow is spread not only into the integrated heatsink but also into the bonding leads (25  $\mu$ m) on top of the upside-down mounted diode. Single mesa-diodes with diameters between 100 and 200  $\mu$ m for pulse operation in the *V*- and *W*-bands are obtained by standard photoresist technology. The individual diodes with integral Au-Ag-Au heatsinks are soldered on the gold-plated stud and quartz standoffs, as well as quartz and ceramic rings of various sizes, which are used for different mounting techniques. Hereby, the parasitic capacitance and inductance of the mounted devices can be varied in order to achieve optimum matching to the resonator.

### III. MILLIMETER-WAVE CIRCUIT

At millimeter-wave frequencies, inductive-post or cap-type waveguide resonators are commonly used. The latter have been applied with great success in this laboratory for frequencies up to 140 GHz for CW IMPATT diodes mounted with very low parasitic capacitance and inductance [9], [10]. Single-drift pulsed IMPATT diodes mounted also with very low parasitics deliver about 5-W output power at *V*-band frequencies if they are operated in either a cap structure or an inductive-post resonator. Fig. 1 shows the cross section of an inductive-post resonator with reduced waveguide height. A detailed theoretical description of this resonator is given by Williamson [8] for low frequencies up to *Ku*-band and is adopted also for *V*-band frequencies. The diode is mounted on the bottom of the waveguide floor and the bias is provided through a choke with the inductive post. A sliding short behind the diode allows proper frequency and maximum output power tuning. Additionally, for impedance matching of the diode and the resonator, the post radius  $r_c$  and the length  $l_c$  of the coaxial section can be varied. The waveguide height is reduced and a taper connects the resonator with the WR-15 waveguide measuring system. Taking into account perfect matching at both waveguide arms and, for example  $l_c = 0$ , the real and imaginary parts of the circuit impedance  $Z_c$  presented to the diode are plotted in Fig. 2 as functions of the reduced waveguide height  $b$ .